Proceedings of the 2000 IEEE
International Conference on Robotics & Automation
San Francisco, CA • April 2000

Robot Acceleration Capability: The Actuation Efficiency Measure

Alan Bowling Oussama Khatib
Robotics Laboratory
Department of Computer Science
Stanford University, Stanford, CA 94086

Abstract

This article presents a new performance measure, the actuation efficiency, which describes isotropy in acceleration capability for non-redundant manipulators. It measures the imbalance between the end-effector accelerations achievable in different directions. Prior to this, no measure of this characteristic was adequate for a six degree-of-freedom manipulator, because its end-effector motions are referenced to a mix of linear and angular coordinates. The proposed measure addresses both linear and angular accelerations. It also indicates oversized actuators, since this contributes to the imbalance in achievable accelerations. The development of this measure is based on the formulation of the motion isotropy hypersurface. The shape of this hypersurface is a weak indicator of acceleration isotropy.

1 Introduction

A balanced or isotropic performance is a characteristic of manipulators which are well suited for general tasks. This means that its abilities are the same in all directions. These mechanisms are more versatile and adaptable to different, more complex tasks, as opposed to those designed for a specific task or motion. This article examines *acceleration capability*, which refers to a manipulator's ability to accelerate its end-effector. This determines how quickly it can manipulate grasped objects, and its responsiveness to controller commands. For general tasks, acceleration capability is considered to be limited by the weakest acceleration achievable in some direction. This is measured by the *isotropic acceleration*, which is the largest magnitude of end-effector acceleration achievable in every direction. However, it does not describe the imbalance, or anisotropy, between the accelerations achievable in different directions; e.g. between the largest and smallest accelerations. This characteristic is referred to as *acceleration isotropy*. Developing a measure for it is the focus of this article. The measure, the *actuation efficiency*, is intended to aid in manipulator design.

The study of acceleration isotropy begins by examining the isotropic acceleration. A number of studies have explored the isotropic acceleration and other ways of characterizing end-effector accelerations. To name a few, in 1985 Yoshikawa [1, 2] developed the the *dynamic manipulability ellipsoid*, which led to the *dynamic manipulability measure* and the isotropic acceleration. Kosuge and Furuta [3] proposed the use of the condition numbers of the Jacobian and a weighted inertia tensor as measures of isotropy. Thomas, Yuen-Chow and Tesar [4] developed an actuator selection algorithm based on the isotropic acceleration. In 1987 Khatib and Burdick proposed the *acceleration hyperparallelipiped* which yields the isotropic acceleration. In 1988 Graettinger and Krogh [5] proposed the *acceleration radius*, which described the isotropic acceleration over the workspace. In 1989 Kim and Desa developed *acceleration set theory* [6, 7] for determining the isotropic accelerations. Many other studies followed these same lines [8, 9].

However, these earlier studies did not adequately deal with the inhomogeneities, or difference in units, between the properties related to linear and angular motion. This limited their utility to mechanisms with three or fewer degrees-of-freedom (DOF). This problem was discussed extensively by Doty, Melchiorri, Schwartz, and Bonivento [10, 11]. The *motion isotropy hypersurface* [12] was one of the first characterizations to provide a complete description of the linear and angular isotropic accelerations for a six DOF non-redundant manipulator. The development of the motion isotropy hypersurface also leads to the proposed measure. Thus the actuation efficiency also considers both accelerations.

0-7803-5886-4/00/$10.00© 2000 IEEE

The measure is defined as the ratio of useful to available torque. "Useful" refers to the torques which contribute to the isotropic accelerations. The remaining torque serves to increase the imbalance in achievable accelerations. The amount of extra torque capacity depends on the mechanism's dynamics and the actuator torque capacities. The measure indicates when changes in these two areas could improve acceleration isotropy. It is especially useful for sizing actuators.

This article focuses on local isotropy determined at a particular configuration, for non-redundant manipulators. In the next sections a brief discussion of the isotropic accelerations is presented first. This is followed by the development of the actuation efficiency. The relationship between the actuation efficiency and the motion isotropy hypersurface is also discussed. The measure is then evaluated and used for the redesign of the PUMA 560 manipulator.

2 Understanding Acceleration Isotropy

The study of the isotropic accelerations facilitates understanding acceleration isotropy. This investigation involves the relationship between the bounds on actuator torque capacity and end-effector acceleration, which is developed from the equations of motion,

$$A(\mathbf{q})\,\ddot{\mathbf{q}} + \mathbf{b}(\dot{\mathbf{q}},\mathbf{q}) + \mathbf{g}(\mathbf{q}) = \boldsymbol{\Gamma}(\mathbf{q}) = \mathbf{G}^T(\mathbf{q})\,\boldsymbol{\Upsilon}, \quad (1)$$

the Jacobian,

$$\begin{bmatrix} \boldsymbol{v} \\ \boldsymbol{\omega} \end{bmatrix} = J(\mathbf{q})\,\dot{\mathbf{q}}, \quad (2)$$

and the bounds on the actuator torque capacities,

$$-\boldsymbol{\Upsilon}_{bound} \le \boldsymbol{\Upsilon} \le \boldsymbol{\Upsilon}_{bound}. \quad (3)$$

In equation (1), $\mathbf{q}$ is the vector of joint/generalized coordinates. A, $\mathbf{b}$, and $\mathbf{g}$ are the inertia tensor, Coriolis and centrifugal forces, and gravity forces. The matrix $\mathbf{G}$ describes the transmission system which translates actuator torques, $\boldsymbol{\Upsilon}$, into joint torques, $\boldsymbol{\Gamma}$. In equation (2), $\boldsymbol{v}$ and $\boldsymbol{\omega}$ are the linear and angular end-effector velocities, and J is the Jacobian.

Omitting the velocity dependent terms, equations (1) through (3) are used to obtain

$$-\mathbf{1} \le E_v\dot{\boldsymbol{v}} + E_\omega\dot{\boldsymbol{\omega}} + N\mathbf{G}^{-T}\mathbf{g} \le \mathbf{1} \quad (4)$$

where

$$E = [\,E_v\;E_\omega\,] = N\,\mathbf{G}^{-T}\,A\,J^{-1}. \quad (5)$$

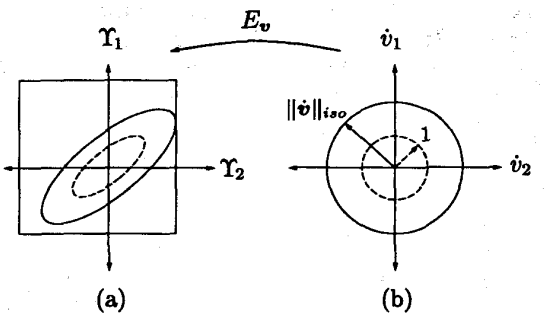

Figure 1: 2 DOF Isotropic Acceleration. The isotropic acceleration circle is mapped into a torque ellipse which is expanded/contracted until it touches the bounds.

The reader is referred to [12] for the details. Equation (4) has been normalized by the actuator torque capacities contained in the diagonal matrix N with $N_{ii} = \frac{1}{\Upsilon_{bound_i}}$, resulting in bounds equal to one.

The isotropic accelerations are determined by visualizing the terms in equation (4) as geometric objects, and exploring the relationships between them. For instance, the bounds are considered as an n-dimensional hypercube where each side has a length of two. At a particular configuration, the gravity term is constant and can be subtracted from the bounds, thereby shifting them away from the origin. This is shown in Figure 1a for a simple two DOF planar manipulator.

First, consider the linear isotropic acceleration described by the sphere

$$\dot{\boldsymbol{v}}^T\dot{\boldsymbol{v}} = \|\dot{\boldsymbol{v}}\|^2. \quad (6)$$

The largest value of $\|\dot{\boldsymbol{v}}\|$ is determined by examining the sphere's image in torque space, which is obtained using E_v from equation (4),

$$\boldsymbol{\Upsilon}_v^T\,(\,E_vE_v^T\,)^+\,\boldsymbol{\Upsilon}_v = \|\dot{\boldsymbol{v}}\|^2 \quad (7)$$

where the superscript + indicates the Moore-Penrose psuedoinverse.

This ellipsoid is mapped to the origin of the torque bounds. Then, beginning with $\|\dot{\boldsymbol{v}}\| = 1$, the ellipsoid is expanded/contracted, by changing $\|\dot{\boldsymbol{v}}\|$, until it first touches and lies within the torque bounds. The value of $\|\dot{\boldsymbol{v}}\|$ at which this occurs determines the linear isotropic acceleration $\|\dot{\boldsymbol{v}}\|_{iso}$; see Figure 1.

The directions in which the ellipsoid does not touch the bounds indicate where there is more torque capacity available for achieving higher accelerations. Figure 1a shows a large imbalance in the amount of acceleration

achievable in different directions. However, *it is impossible to attain perfect acceleration isotropy, because the ellipsoid cannot simultaneously lie within and completely encompass the torque bounds.*

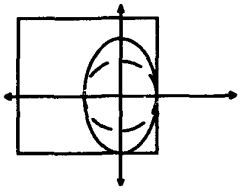

Figure 2: Ideal Isotropy. The ellipse encompasses more volume than the inscribed circle.

A more balanced acceleration capability is obtained when *the $\|\dot{v}\|_{iso}$ torque ellipsoid occupies as much volume within the torque bounds as possible.* Note that the ideal shape of the torque ellipsoid is not a sphere, because the bounds are shifted away from the origin due to gravity. For example, Figure 2 shows an ellipse that occupies more volume of the shifted torque bounds than the inscribed circle. Notice that the gravity shift makes portions of torque bounds unusable for producing isotropic acceleration. Also note that the condition number of E_v is seldom useful for measuring acceleration isotropy, since it only describes the proximity of the ellipsoid to a sphere. The inscribed ellipsoid will be used to compute the available torque reference.

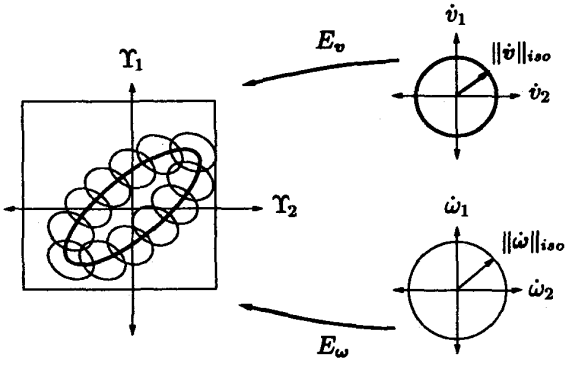

Figure 3: Torque Ellipse Addition. The isotropic linear and angular accelerations are mapped into torque ellipsoids and added to form a composite surface.

Now consider both the linear and angular isotropic accelerations. As in the linear case, a torque ellipsoid representing the angular isotropic acceleration can be developed by transforming the sphere,

$$\dot{\omega}^T\dot{\omega} = \|\dot{\omega}\|^2, \tag{8}$$

using E_ω from equation (4) into,

$$\Upsilon_\omega^T \left(E_\omega E_\omega^T \right)^+ \Upsilon_\omega = \|\dot{\omega}\|^2. \tag{9}$$

The addition of the linear and angular acceleration terms in equation (4) is accomplished by mapping the center of one ellipsoid onto every point on the surface of the other. This is valid because both ellipsoids are described in terms of torque vectors in the same space. In short, two unlike quantities are transformed into two like quantities so that they may be added. This addition is difficult to illustrate in general, so an approximation to it is shown in Figure 3.

The composite surface formed by this addition is expanded or contracted until it first touches and lies completely within the bounds. However, there are many surfaces which satisfy this condition. The solutions are represented by a convex, piecewise linear curve, the *motion isotropy curve* of Figure 4. It gives the sizes of the ellipsoids in the solution set. The curve shows a tradeoff between how much torque is used to produce linear and angular isotropic accelerations. The actuator which saturated providing the level of performance along a line segment, referred to as the *limiting actuator(s)*, is indicated by a numeric label.

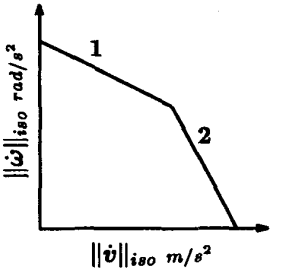

Figure 4: Motion Isotropy Curve. The relationship between the linear and angular isotropic accelerations.

The motion isotropy curve is described by

$$\mathbb{A}\begin{bmatrix} \|\dot{v}\| \\ \|\dot{\omega}\| \end{bmatrix} \leq \mathbb{T} = \begin{bmatrix} 1 - NG^{-T}\mathbf{g} \\ 1 + NG^{-T}\mathbf{g} \end{bmatrix} \tag{10}$$

obtained from equations (1) through (3), see [12]. Assuming that the manipulator has n actuators, $\mathbb{A}$ is a $2n \times 2$ matrix where

$$\begin{matrix} \mathbb{A}_{1,i} \\ \text{and} \\ \mathbb{A}_{1,i+n} \end{matrix} = \sqrt{\sum_{j=1}^{r} E_{ij}} \qquad \begin{matrix} \mathbb{A}_{2,i} \\ \text{and} \\ \mathbb{A}_{2,i+n} \end{matrix} = \sqrt{\sum_{j=r+1}^{n} E_{ij}} \tag{11}$$

The lines represented by these relations are overlayed in the same space, and the innermost envelope formed by them is the motion isotropy curve of Figure 4.

3 The Actuation Efficiency

The actuation efficiency, η, is based on the total volume encompassed by the union of *all* of the composite

surfaces described by the motion isotropy curve. For instance, this volume would resemble a cylinder for a three DOF planar manipulator. This is then divided by the volume of the hyperellipsoid inscribed within the torque bounds, similar to the one in Figure 2. In practice, these volumes are not difficult to determine. The next sections briefly discuss these computations.

3.1 Volume of Composite Surfaces

The volume within the composite surfaces is iterpreted as the useful torque, V_{useful},

$$V_{useful} = \int_V dV. \tag{12}$$

This integral is not difficult to evaluate because a simple cross-sectional element, the volume of one ellipsoid, can be defined. This volume is evaluated using spherical coordinates. These are $y_1 = \|\dot{\omega}\|\lambda_1 \sin(\phi)\cos(\theta)$, $y_2 = \|\dot{\omega}\|\lambda_2 \sin(\phi)\sin(\theta)$, and $y_3 = \|\dot{\omega}\|\lambda_3 \cos(\phi)$ where y_1, y_2, and y_3 are the ellipsoid's principal axes, and the λ's are the singular values of E_ω. Its volume, v_ω, is

$$\mathrm{v}_\omega(\|\dot{v}\|) = \frac{4\pi}{3}\lambda_1\lambda_2\lambda_3(m\|\dot{v}\| + c)^3 \tag{13}$$

which resembles the familiar ellipsoid volume formula, except for the radius $\|\dot{\omega}\| = m\|\dot{v}\| + c$. Recall that $\|\dot{\omega}\|$ is dependent on $\|\dot{v}\|$, as described by the motion isotropy curve, Figure 5. Since the curve is piecewise linear, the overall integral is evaluated in segments.

Using equation (12) and (13), the useful volume obtained from one line segment of the motion isotropy curve, v_{useful}, can be expressed as [13]

$$\mathrm{v}_{useful} = \int\int\int \mathrm{v}_\omega(\|\dot{v}\|)\, dx_1\, dx_2\, dx_3 \tag{14}$$

where x_1, x_2, and x_3 are coordinates orthogonal to each other and to the principal axes of the E_ω ellipsoid. The region over which to integrate v_ω is determined by projecting the E_v ellipsoid onto x_1, x_2, and x_3. This is accomplished using the *orthogonal projector* matrix P_ω to obtain,

$$\Upsilon_x = P_\omega\, \Upsilon_v = P_\omega\, E_v\, \dot{v} \tag{15}$$

$$= \left[\, \mathrm{I} - \left(E_\omega E_\omega^+ \right)^T \right] E_v\, \dot{v} \tag{16}$$

where I is the appropriately dimensioned identity matrix. Combining equations (6) and (15) yields

$$\Upsilon_x^T \left(P_\omega\, E_v\, E_v^T\, P_\omega^T \right)^+ \Upsilon_x = \|\dot{v}\|^2 \tag{17}$$

whose principal axes are x_1, x_2, and x_3.

Using spherical coordinates, equation (14) becomes

$$\frac{\mathrm{v}_{useful}}{\lambda_4\lambda_5\lambda_6} = \int_a^b \int_0^\pi \int_0^{2\pi} \mathrm{v}_\omega(\|\dot{v}\|)\|\dot{v}\|^2 \sin(\phi)\, d\theta\, d\phi\, d\|\dot{v}\| \tag{18}$$

where λ_4 through λ_6 are the singular values of $(P_\omega E_v)$, and a and b are the maximum and minimum values of $\|\dot{v}\|_{iso}$ along a segment of the motion isotropy curve, as shown in Figure 5.

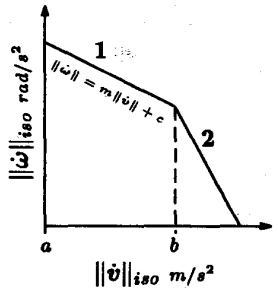

Figure 5: Motion Isotropy Curve. a and b values, and the equation for the first line segment of the curve.

In the six DOF case, the integrand in equation (18) is a polynomial whose antiderivative is

$$F_{33}(\|\dot{v}\|) = \frac{8\pi^2}{3}\lambda_1 \cdots \lambda_6\|\dot{v}\|^3 \left(\frac{m^3}{6}\|\dot{v}\|^3 + \frac{3m^2c}{5}\|\dot{v}\|^2 + \frac{3mc^2}{4}\|\dot{v}\| + \frac{c^3}{3} \right) \tag{19}$$

where the subscript "33" denotes the dimensions of v and ω, in no particular order. In general,

$$\mathrm{v}_{useful}(a, b) = F_{v\omega}(b) - F_{v\omega}(a), \tag{20}$$

and therefore equation (12) becomes

$$V_{useful} = \sum_{i=1}^{z} \mathrm{v}_{useful}(a_i, b_i, c_i, m_i) \tag{21}$$

where z is the number of piecewise linear segments comprising the motion isotropy curve. Note that the λ's are the singular values of E_ω and $P_\omega E_v$, $a_i \le \|\dot{v}\| \le b_i$, c_i is the $\|\dot{\omega}\|_{iso}$-intercept, and m_i is the slope of the line segment. $F_{v\omega} = F_{\omega v}$, for mechanisms with fewer than six DOF;

$$\begin{aligned} F_{32} &= 4\pi^2\lambda_1 \cdots \lambda_5\|\dot{v}\|^3 \left(\frac{m^2}{5}\|\dot{v}\|^2 + \frac{mc}{2}\|\dot{v}\| + \frac{c^2}{3} \right) \\ F_{31} &= 8\pi\lambda_1 \cdots \lambda_4\|\dot{v}\|^3 \left(\frac{m}{4}\|\dot{v}\| + \frac{c}{3} \right) \\ F_{22} &= 4\pi^2\lambda_1 \cdots \lambda_4\|\dot{v}\|^2 \left(\frac{m^2}{4}\|\dot{v}\|^2 + \frac{2mc}{3}\|\dot{v}\| + \frac{c^2}{2} \right) \\ F_{21} &= 4\pi\lambda_1 \cdots \lambda_3\|\dot{v}\|^2 \left(\frac{m}{3}\|\dot{v}\| + \frac{c}{2} \right). \end{aligned} \tag{22}$$

3.2 Inscribed Hyperellipsoid Volume

Since perfect acceleration isotropy is unattainable, the unusable portions of the torque bounds are discarded

from the available torque. The simplest way to do this is to use the volume, $V_{available}$, of the hyperellipsoid inscribed within the bounds, whose principal axes align with the coordinate axes. The lengths of the principal axes are determined from the gravity shifted bound vectors contained in $\mathbb{T}$, equation (10), as the element with smallest absolute value for each direction. The volume of this hyperellipsoid for different dimensions is given in Table 1, where the λ's indicate the lengths of the principal axes.

$$V_{available} = d \prod_{i=1}^{n} \lambda_i$$

n	1	2	3	4	5	6
d	2	π	$\frac{4\pi}{3}$	$\frac{\pi^2}{2}$	$\frac{8\pi^2}{15}$	$\frac{\pi^3}{6}$

Table 1: Inscribed Hyperellipsoid Volume

The actuation efficiency, η, is written as a percentage,

$$\eta = \frac{V_{useful}}{V_{available}}. \tag{23}$$

4 The Motion Isotropy Curve and η

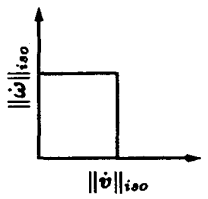

Figure 6: Isotropy Indicator. Rectangle suggests high degree of acceleration isotropy.

The shape of the motion isotropy curve is a weak indicator of acceleration isotropy. The closer the curve is to forming a rectangle with the coordinate axes, the more likely it is that a high degree of acceleration isotropy exists at that configuration. If the motion isotropy curve forms a perfect rectangle with the coordinate axes, Figure 6, $\|\dot{v}\|$ and $\|\dot{\omega}\|$ are independent. Thus both attain their maximum values within the bounds, yielding a composite surface which engulfs all of the other possible surface sizes specified by the curve. This is a weak indication that the mechanism has a high degree of acceleration isotropy. However, η must still be calculated, since the shape of the ellipsoids, not described by the curve, must be considered.

If the motion isotropy curve forms something closer to a triangle with the coordinate axes, as in Figure 4, this indicates a tradeoff between $\|\dot{v}\|$ and $\|\dot{\omega}\|$; when one increases the other must decrease. This reduces the possible volume of each composite surface, and thus the manipulator should have a lesser degree of acceleration isotropy.

5 Application

Figures 7a and 7b show two configurations of the PUMA 560 which have different actuation efficiencies, computed for an operational point located at the intersection of the three wrist rotation axes. Initially the actuation efficiencies are 38% and 10%. These values indicate a large imbalance between the end-effector accelerations achievable in different directions, which may be caused by oversized actuators.

The motion isotropy curves for these two configurations, Figure 7c, tell which actuator may be suspect. Notice that for these configurations, the closer the motion isotropy curve is to a rectangle, the higher the acceleration isotropy, as discussed in Section 4. The limiting actuators indicated in Figure 7c are 1, 2, 5, and 6. Therefore actuators 3 and 4 are candidates for change. The limiting actuators also suggest which motors can be changed to increase performance. Reducing the peak torque of the third actuator by half, from $1.6Nm$ to $0.8Nm$, results in new actuation efficiencies of 78% and 29%, a more than two-fold increase in acceleration isotropy for both configurations.

This actuator change neither reduces nor alters the manipulator's isotropic accelerations, given in Figure 7c. This implies that the lesser actuation efficiencies were partially due to an oversized third actuator. Recall that the shape of the ellipsoids, determined by the mechanism's dynamics, should also be considered. Reducing the size of third actuator could result in less weight for the manipulator to carry while in motion, which can lead to a better overall performance.

6 Conclusion

This article presented a new measure, the actuation efficiency, which describes the imbalance between the end-effector accelerations achievable in different directions. It also indicates possible actuator oversizing, since this contributes to the imbalance in acceleration capability. The measure includes both linear and angular accelerations in its description of acceleration isotropy. This allows for the analysis of a non-redundant manipulator having up to a full six

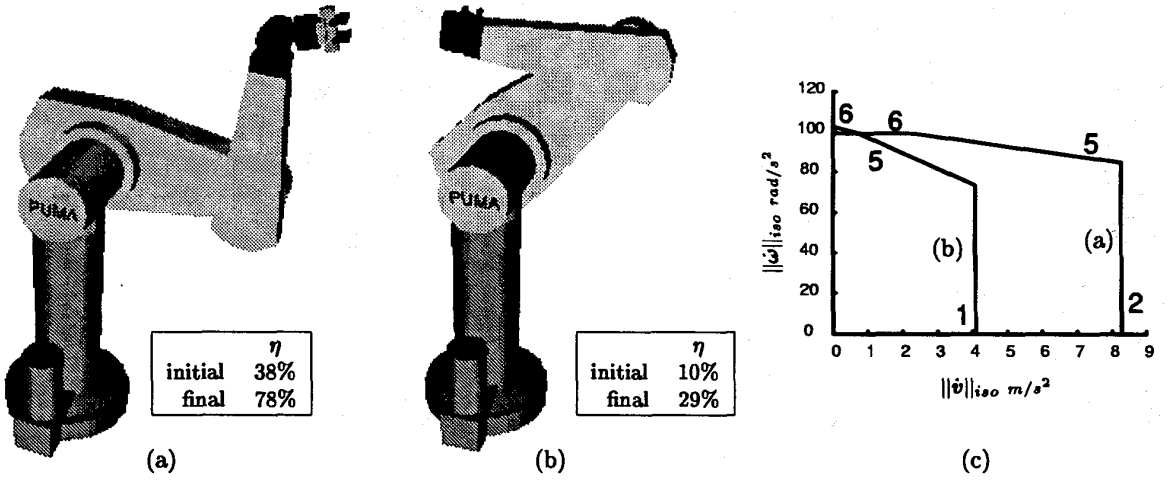

Figure 7: PUMA 560 Actuation Efficiencies and Motion Isotropy Curves.
Reducing the peak torque of the third actuator yields a more than two-fold increase in acceleration isotropy for both configurations without sacrificing isotropic performance.

DOF. This article also establishes the shape of the motion isotropy curve as a weak indicator of acceleration isotropy. It concludes with a design example involving the PUMA 560 manipulator. A similar measure can be developed for force capability, which describes a manipulator's ability to apply forces and moments to the environment at the end-effector. Future work involves using this measure in design optimizations, and investigating ways of describing acceleration isotropy for the entire workspace.

References

[1] Tsuneo Yoshikawa. Dynamic manipulability of robot manipulators. In *Proceedings 1985 IEEE International Conference on Robotics and Automation*, pages 1033–1038, 1985. St. Louis, Missouri.

[2] Tsuneo Yoshikawa. Dynamic manipulability of articulated robot arms. In *15th International Symposium on Industrial Robots*, pages 865–872, September 1985.

[3] Kazuhiro Kosuge and Katsuhisa Furuta. Kinematic and dynamic analysis of robot arm. In *Proceedings IEEE International Conference on Robotics and Automation*, volume 2, pages 1039–1044, 1985.

[4] M. Thomas, H. C. Yuan-Chou, and D. Tesar. Optimal actuator sizing for robotic manipulators based on local dynamic criteria. *Transactions of the ASME Journal of Mechanisms, Transmissions, and Automation in Design*, 107(2):163–169, 1985.

[5] Timothy J. Graettinger and Bruce H. Krogh. The acceleration radius: A global performance measure for robotic manipulators. *IEEE Journal of Robotics and Automation*, 4(1):60–69, February 1988.

[6] Yong-Yil Kim and Subhas Desa. The definition, determination, and characterization of acceleration sets for spatial manipulators. In *The 21st Biennial Mechanisms Conference: Flexible Mechanism, Dynamics, and Robot Trajectories*, pages 199–205, September 1990. Chicago, Illinois.

[7] Y. Kim and S. Desa. The definition, determination, and characterization of acceleration sets for spatial manipulators. *The International Journal of Robotics Research*, 12(6):572–587, 1993.

[8] Ou Ma and Jorge Angeles. The concept of dynamic isotropy and its applications to inverse kinematics and trajectory planning. In *Proceedings IEEE International Conference on Robotics and Automation*, volume 1, pages 481–486, 1990.

[9] Zhanfang Zhao, Zhen Wu, Jilian Lu, Weihai Chen, and Guanghua Zong. Dynamic dexterity of redundant manipulators. In *Proceedings IEEE International Conference on Robotics and Automation*, volume 2, pages 928–933, 1995.

[10] Keith L. Doty, Claudio Melchiorri, and Claudio Bonivento. A theory of generalized inverses applied to robotics. *The International Journal of Robotics Research*, 12(1):1–19, 1993.

[11] Keith L. Doty, Claudio Melchiorri, Eric M. Schwartz, and Claudio Bonivento. Robot manipulability. *IEEE Transactions on Robotics and Automation*, 11(3):462–468, 1995.

[12] Alan Bowling and Oussama Khatib. The motion isotropy hypersurface: A characterization of acceleration capability. In *Proceedings IEEE/RSJ International Conference on Intelligent Robots and Systems*, volume 2, pages 965–971, October 1998. Victoria, British Columbia, Canada.

[13] Jerrold E. Marsden and Anthony J. Tromba. *Vector Calculus*. John Wiley & Sons, second edition, 1976.